Vergara Lourencon, Tainise; Garcia Greca, Luiz; Tarasov, Dmitry; Borrega, Marc; Tamminen, Tarja; Rojas Gaona, Orlando; Balakshin, Mikhail

Lignin-first integrated hydrothermal treatment (HTT) and synthesis of low-cost biorefinery particles

Published in:
ACS Sustainable Chemistry and Engineering

DOI:
10.1021/acssuschemeng.9b06511

Published: 21/01/2020

Document Version
Peer-reviewed accepted author manuscript, also known as Final accepted manuscript or Post-print

Please cite the original version:
Vergara Lourencon, T., Garcia Greca, L., Tarasov, D., Borrega, M., Tamminen, T., Rojas Gaona, O., & Balakshin, M. (2020). Lignin-first integrated hydrothermal treatment (HTT) and synthesis of low-cost biorefinery particles. *ACS Sustainable Chemistry and Engineering*, *8*(2), 1230-1239. https://doi.org/10.1021/acssuschemeng.9b06511

Lignin-first integrated hydrothermal treatment (HTT) and synthesis of low-cost biorefinery particles

Tainise V. Lourencon[†], *Luiz G. Greca*[†], *Dmitry Tarasov*[†], *Marc Borrega*[‡], *Tarja Tamminen*[‡], *Orlando J. Rojas*[†], *Mikhail Y. Balakshin*[†*]

[†]Department of Bioproducts and Biosystems, School of Chemical Engineering, Aalto University, P.O. Box 16300, 00076, Finland

[‡]VTT Technical Research Centre of Finland, P.O. Box 1000, 02044 Espoo, Finland

ABSTRACT

Hydrothermal treatments (HTT) are used in the biorefineries to effectively valorize carbohydrate fractions and their products. However, lignin is often marginalized as a secondary component. Herein, we propose a new biorefinery approach focused on lignin valorization. We demonstrate that high-value lignins can be extracted using a simple, green and affordable process consisting of an optimized HTT followed by lignin extraction with aqueous acetone under ambient conditions. Significantly, the chemical structure and molecular mass of the lignin can be tailored by the selection of the process variables while maintaining a high yield, in the range of ~ 60-90%. For example, the average molecular mass (Mw) of the isolated lignins is in the range between 2.5 and 5 kDa while the amount of β-O-4 linkages is 4-28 per 100 Ar. The extracted lignins are further used to generate micro and nanoparticles by using an aerosol flow system. The introduced lignin profiling affords control of particle properties, including average size and distribution, surface energy and wettability. Overall, the suggested approach allows to customize lignin products while achieving a 58% reduction in the lignin particles production costs compared to the lowest prime figures reported so far.

KEYWORDS**:** Autohydrolysis, Biorefinery, Lignin valorization, Lignocellulose, Nanoparticles

INTRODUCTION

The exploration of natural sources to mitigate our dependency on fossil-based fuels and raw materials has been motived by the gradual depletion of fossil feedstock and the variability of crude oil prices. Such factors are coupled with the growth in population and related basic needs.[1] In this sense, lignocellulosic biomass is a suitable alternative, especially given its abundance as a source of organic carbon available.[2,3] For conversion and utilization of biomass to value-added products, such as biofuels, bio-based chemicals and materials, the lignocellulosic biorefinery (LCB) concept has received a great attention.[4]

Among common biorefinery processes, hydrothermal treatment (HTT), also known as autohydrolysis, stands as an environmentally friendly and cost-efficient technology for the extraction of hemicelluloses from biomass. HTT is also distinctive for its flexibility and simplicity.[5,6] The simple use of water in HTT, removing the need for extra chemicals in the reaction medium, is the principal foremost advantage of this process.[5,7] HTT has been used in the pulping industry for the production of dissolving grade pulps,[8] as well as in emerging sugar-based biorefineries for the optimization of hemicellulose extraction[9,10] and for the adjustment of the reactivity of cellulose-rich solids for further enzymatic hydrolysis.[11,12] Therefore, all efforts in HTT-based biorefineries have focused on the optimization of the conditions for carbohydrates valorization.[13,14] However, the biorefinery lignins, generated in this (and other) process, have been traditionally considered as a side-streams,[15] mostly for uses in low-value applications; hence, they have been disregarded in efforts related to process optimization.

Given the importance of lignin as an abundant natural resource, potentially available in large quantities from pulping industries and LCB,[16–18] its valorization into industrially relevant products depends on a comprehensive investigation of lignin isolation, and obtained structures and properties.[19,20]

A few works have reported lignin extraction from biorefinery solids. Sun et al.[21] extracted about 50% lignin from hydrothermally-treated eucalyptus fiber with aqueous NaOH. Li et al[22] extracted 26-50% of lignin from steam exploded solids of aspen wood with dioxane/water. Four decades ago Lora and Wayman[23] investigated lignin extraction with dioxane/water solutions from hydrothermally-treated hardwoods. In this latter work, hardwood chips and sawdust were subjected to HTT at temperatures of 175-220˚C at liquid to solid (L/S) ratio of 1. It was reported that application of aqueous dioxane solution under reflux allowed extraction of up to 91.6% of the original lignin from HTT-pretreated hardwoods. Also, 98% of lignin could be extracted after boiling the HTT- solids for 3 hours in 1% NaOH solution; however, this also resulted in the extraction of half of the original wood cellulose. Unfortunately, dioxane is not an industrially feasible solvent while NaOH extraction is bound to generate undesirable carbohydrate side products. In addition, the structure and properties of the extracted lignins were not reported.

Inspired by the work of Lora and Wyman we explored the feasibility of a process with industrial viability. Specifically, we focus on an HTT-based biorefinery concept to extract high-value lignins from hardwood (birch) by using an aqueous acetone solution under ambient conditions. Our main objective is to evaluate the yield and the properties of the lignins isolated from the pre-treated biomass under respective HTT conditions.

In addition, the assembly of lignin into micro/nanoscaled structures makes it possible to improve the properties of the materials by taking advantage of lignin's inherent molecular structure and composition, opening a wide range of applications.[24,25] Thus, the integrated production of dry lignin micro/nanoparticles (LMNP) is proposed by using the dissolved lignins directly (i.e. without lignin precipitation and drying) through an aerosol flow system, resulting in substantially lower production costs than the ones previously reported for such method.

MATERIAL AND METHODS

Wood material. Chips of birch wood (*Betula sp.*) were ground into sawdust and screened (0.55–0.125 mm particle size). Acetone extraction of the sawdust prior to hydrothermal treatments was used to eliminate the effect of wood lipophilic extractives in order to understand better the lignin fundamentals in the process.

Hydrothermal Treatment (HTT). The hydrothermal treatments (**Figure 1**) were conducted in a 50 mL batch reactor (Parr Reactor 4841), equipped with a temperature controller, a pressure gauge and a mechanical stirrer. About 4.2 g (per dry mass) of the extractives-free birch sawdust was placed in the reactor and then filled with deionized water, reaching distinct L/S ratio. The effect of HTT parameters on lignin removal and extracted-solids were evaluated by processing temperature and residence time which were combined in the P-factor value by assuming an Arrhenius-type equation with an activation energy of 125.6 kJ/mol.[26] Severity factors are also provided in **Table S3** to allow an easily comparison of the current data with published literature. Once a target P-factor was reached, the autoclave was immediately cooled in an ice bath to prevent further reactions. The HTT profiles can be seen in **Figure S1**. Then, the reaction mixture was transferred to a filtering crucible and vacuum-filtered. The produced liquor (hydrolysate) was collected for the subsequent analyses. Hydrothermally treated solids were thoroughly washed with deionized water and then extracted with acetone/water 9/1 (v/v) solution at room temperature, until yielding a colorless filtrate. The extracted solids were collected and dried at 105˚C for 24 h. The solution containing the acetone-extracted lignin (AEL) was collected and concentrated in a rotary evaporator at 40˚C for further characterization. Replicates of AEL at P-factor=2000 and L/S=4, were dried directly as lignin micro/nanoparticles (LNMP), as shown in **Figure 1c**.

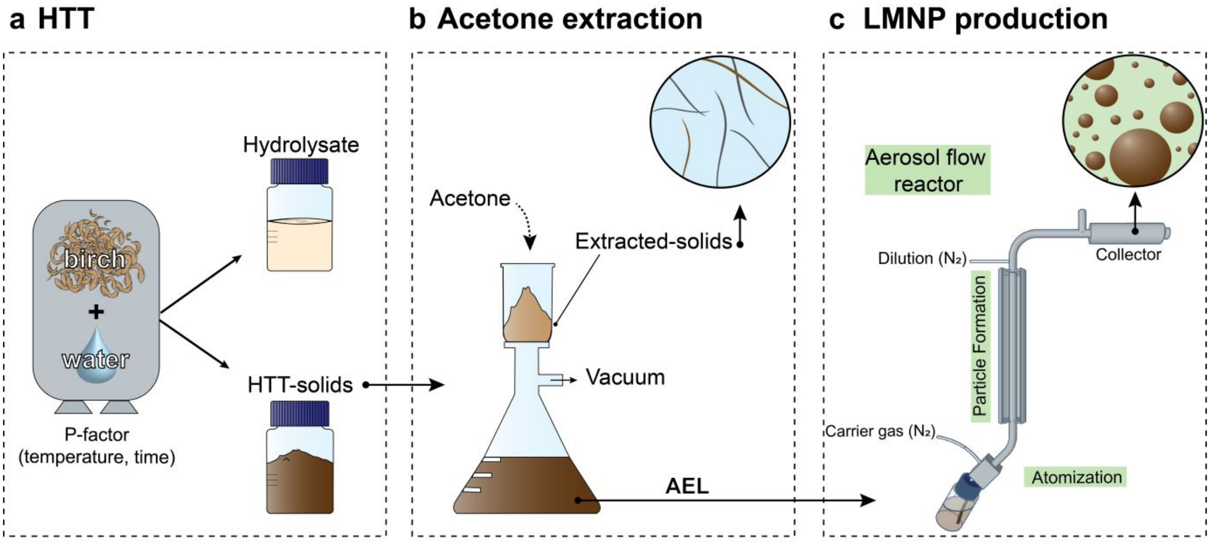

Figure 1. Scheme of the experimental design. (a) Hydrothermal treatment of birch sawdust and the two resulted products: hydrolysate and HTT-solids; (b) lignin extraction from HTT-solids with aqueous acetone, generating the acetone-extracted lignin (AEL) solution and the extracted-solids; (c) controlled drying of AEL, where dried lignin micro/nanoparticles (LMNP) are produced.

Compositional analysis of the feedstock and extracted solids. To determine carbohydrate and lignin contents in the initial material and extracted solids, the samples were subjected to a Saeman hydrolysis - according to a modified NREL procedure - and the resulting neutral monosaccharides were determined by high performance anion exchange chromatography with pulse amperometric detection (HPAEC-PAD) in a Dionex ICS 3000A system equipped with CarboPac PA1 column. The acid insoluble (Klason) lignin content was determined gravimetrically, and the acid soluble lignin was quantified by ultraviolet spectroscopy at 215 and 280 nm as described by Goldschmid (1971).[27] Overall composition and yields of feedstock, solids and AEL can be seen in **Table S1**.

AEL characterization. The AEL extracted from the HTT solids produced at L/S = 4 and 195°C using a P-factor of 500, 800, 1500, 2000 and 2500, were labeled as AEL-1, AEL-2, AEL-3, AEL-4 and AEL-5, respectively. The lignin extracted from solids treated at P-factor of 800 at L/S=8 and 205˚C was denoted as AEL-6. Alcell, a hardwood organosolv (OS), and Indulin AT, a softwood kraft (KL), lignins, were used for comparison.

Molecular weight distribution. The molecular weight distribution of AEL was analyzed by size exclusion chromatography (SEC) after dissolving the sample in 0.1M NaOH (1 mg/mL, pH 13, flow rate 0.5 mL/min, T= 25ºC) using PSS MCX 1000 & 100000 Å columns with a pre-column and Waters 2998 Photodiode Array detector (280 nm). The molecular weight distribution (MWD) were calculated against polystyrene sulphonate (8 x PSS, 1600-148500 g/mol) standards, using Waters Empower 3 software.

Nuclear magnetic resonance (NMR) spectroscopy. The amounts of different hydroxyl groups were determined by ^{31}P NMR spectroscopy[28] (Bruker NMR Spectrometer AV III 400) in accordance with the optimized protocol.[29] Briefly, about 40 mg of dried AEL sample was dissolved in 0.4 ml of a pyridine/deuterated chloroform (1.6/1, v/v) solution. In the next step, 50 µl of chromium (III) acetylacetonate (11.4 mg in 1 mL of the solution) and certain amount of internal standard (IS) (endo-n-hydroxy-5-norbornene-2,3-dicarboximide, 20 mg/ml) required to obtain IS/lignin ratio of 1:20 wt/wt was introduced. Then, 100 µl of phosphorus-containing reagent (2–chloro–4,4,5,5–tetramethyl–1,3,2–dioxaphospholane) was added to the mixture. The vial content was vortexed, transferred into an NMR tube, and submitted for NMR acquisition. The relaxation delay was 5 s and 128 scans were collected. The spectra were phased and calibrated using the signal of water-derivatized product (122.2 ppm). The baseline was corrected using a linear function.

For ^{13}C-NMR analysis,[30] about 200 mg of lignin was dissolved in 0.5 mL solution of DMSO-d_6 containing the relaxation reagent chromium (III) acetylacetonate (6 mg/ml), and the internal standard (IS), trioxane, (40 mg/ml). The ratio of IS/lignin was adjusted to 1:10 wt/wt. The spectra were acquired using 2 s relaxation delay, 1.38 s acquisition time; 20,000 scans were collected. The spectra were processed according to our previous publication.[30]

The HSQC spectra were acquired with approximately 70 mg of lignin dissolved in 0.6 mL of DMSO-d_6. 2D NMR spectra were recorded with a Bruker AVANCE 600 NMR spectrometer with magnetic flux density of 14.1 T, and equipped with a cryogenically cooled 5 mm TCI probe head with inverse geometry (*i.e.*, optimized for proton signal detection). 36 transient (scans per block) were acquired using 1024 data points in F2 (^{1}H) dimension for an acquisition time of 77.8 ms, and 256 data points in F1 (^{13}C) dimension for an acquisition time of 3.94 ms.

The 2D data set was processed with 1024 x 1024 data points using Qsine function in both dimensions. The 2D spectra were quantified using the corresponding quantitative ^{13}C NMR spectra as reference.[31]

Contact Angle measurement. Approximately 150 mg of AEL was used to prepare pellets for static water contact angle (SCA) measurements. The analysis was performed using a KSV Instruments CAM 200 goniometer. The average SCA was determined from 5.5 μL droplets of deionized water placed at three (randomly selected) different positions for each sample. For every measurement of the average SCA, 15 images were recorded from 0 to 15 seconds (at 1 second intervals) after the droplet placement on the pellet.

Dry lignin micro and nanoparticles (LMNP). The AEL was fixed to a concentration of 5% in 90% aqueous acetone and used as precursor solution for LMNP production. The experimental set up used to synthesize the particles was based on a collison-type jet atomizer with nitrogen gas, as the one previously reported by Ago et al.[32] In short, atomized droplets of the lignin solutions were carried through a laminar flow of nitrogen gas (3 L/min) kept at room temperature (25˚C). This process leads to consolidation of droplets into solid particles. In the subsequent section of the reactor, turbulent nitrogen flow at 30 L/min was used for the further removal of residual solvent prior to collection (**Figure 8a**). Afterward, the spherical lignin particles were collected and fractionated by size using a Berner-type low-pressure impactor with 10 different collector stages. In this study, the particles collected at stages 1-7 and 8-10 were combined into two different size populations (small and large, respectively).

Characterization of dry LMNP. The morphology of the lignin particles was analyzed using a field emission scanning electron microscope (FE-SEM, Zeiss Sigma VP, Germany) using an acceleration voltage of 1.6 kV and a working distance of ca. 4.5 mm. Small amounts of the lignin particles were placed on carbon tape and the excess was sample removed with gentle pressurized air. The samples were sputtered using Au-Pd targets to a thickness of ca. 4 nm. The particle size distribution was determined by manually measuring random particles from SEM images by using the image processing ImageJ 2.0.0-rc-68/1.52e. Each size distribution was evaluated from at least 500 measurements. The Zeta potential of the diluted suspensions of the small fraction of the LMNP samples was analyzed by using a Malvern Zetasizer Nano ZS90. The reported values are averages from at least three replicates.

RESULTS AND DISCUSSION

HTT of biomass at L/S ratio 8. The effect of severity (P-factor) was studied at the HTT temperature of 205˚C (optimal one according to Lora and Wayman's work[23]) and L/S=8 (to provide homogenous mixing in the reactor).

As P-factor increased from 800 to 2500, the lignin and xylan content in the extracted solids decreased from 24 to 18% and from 10 to 4%, respectively. The glucan content increased from 57 to 72% (**Figure 2a**).

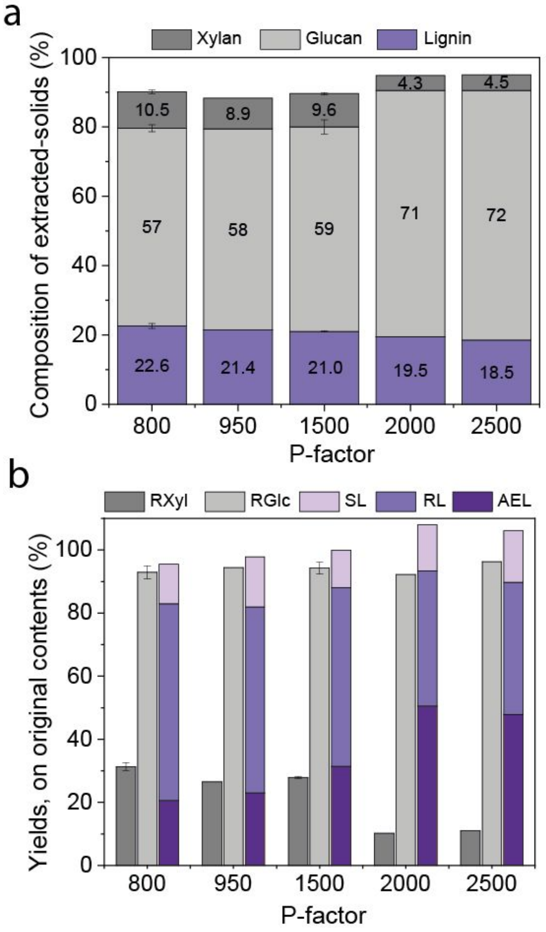

Figure 2. Effect of P-factor at L/S = 8 and 205˚C on the (a) composition of extracted solids and (b) yields measured in the extracted-solids for residual glucan (RGlc), residual xylan (RXyl) and residual lignin (RL). The yields of AEL and soluble lignin (SL in hydrolysate) are also included. All the values were calculated based on the respective content in the original wood feedstock.

Considering the conversion of the biomass components (**Figure 2b)**, approximately 92-96% of the initial glucan (residual glucan, RGlc) remains in the HTT solids in the whole range of P-factor. In contrast, as the P-factor increases the amount of residual xylan (RXyl) decreases from ~30% to 10% (based on the original Xyl content), similarly reported elsewhere.[33]

On the other hand, AEL yields increase with P-factor increment (**Figure 2b**). It can be seen in **Figure 2b** that HTT at P-factor of 2000 allows isolating about 50% (per initial lignin content) via the acetone extraction. Further increase in HTT severity (P-factor of 2500) results in a slight decrease in the AEL yield. The yield of the residual lignin (RL) is the lowest at P-factor =2000, while the amount of lignin soluble in the HTT hydrolysate (soluble lignin, SL) is in the 12-16 % range (**Figure 2b**).

HTT of biomass at L/S ratio 4. It was hypothesized that the limited AEL yield was due to a high L/S ratio; Lora and Wyman obtained significantly higher extraction yields using similar HTT process severity (temperature and time), but at lower L/S ratio. Therefore, the L/S ratio was reduced to 4 at the optimal P-factor of 2000. In particular, the results of HTT at 205˚C and L/S = 4 (**Figure 3**) can be directly compared with those produced at L/S = 8 (**Figure 2**) with the same P-factor (2000) illustrating a very pronounced effect of the L/S ratio.

Effect of the reaction temperature. In the range of temperatures between 175-205˚C (at P-factor= 2000, L/S=4), the contents of xylan in the extracted solids are close to zero (**Figure 3a**). Except for the results at 195˚C, the glucan and lignin content is about 50% and 40%, correspondingly, in all experiments. The HTT extracted solids produced at 195˚C contain much higher glucan (71%) and significantly lower lignin (23%). This fact can be explained by a much more efficient lignin extraction from the HTT solids produced at 195˚C (**Figure 3b**).

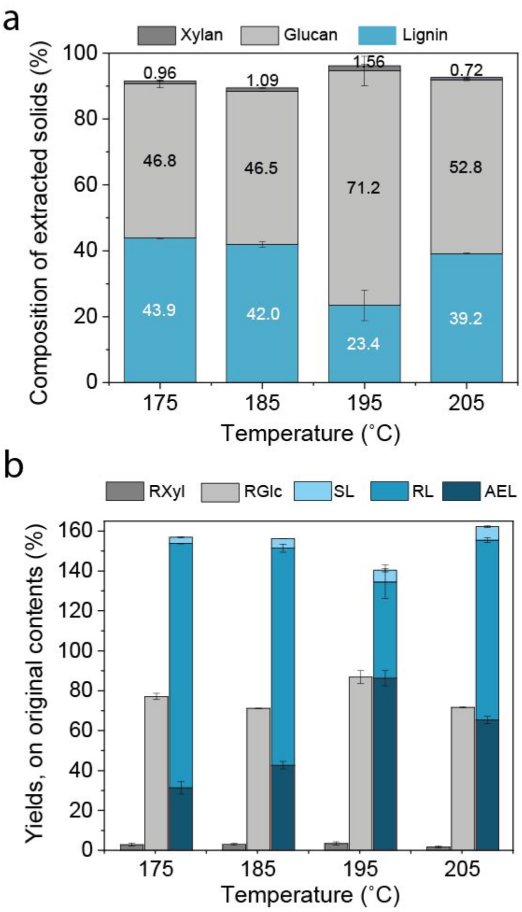

Figure 3. Effect of temperature at L/S=4 and P-factor =2000 on the (a) composition of extracted solids and (b) yields measured in the extracted-solids for RGlc, RXyl and RL. The yields of AEL and SL (in hydrolysate) are also included. All the values were calculated based on the respective content in the original wood feedstock

The dissolution of xylan in HTT at the lower L/S (L/S=4) was almost completed. The amount of RGlc in the extracted-solids was in the range of 70-86% indicating partial degradation of cellulose (**Figure 3b**). This is likely caused by the higher acidity of the hydrolysate with the decrease in the L/S ratio from 8 to 4, due to increase in the solution acidity (organic acid concentration).[9] pH of the hydrolysate was 3.2 and 2.8 at L/S ratios 8 and 4, correspondingly, under comparable HTT conditions (205˚C, P=2000).

Noteworthy, the total lignin amounts (the sum of AEL, RL and SL) were much above 100% (in the range of 140-162%) (**Figure 3b**). This is likely related to the partial conversion of carbohydrate degradation products into products quantified as lignin. This phenomenon is known in industry since 1930s, the so called as ‘humic substances’, ‘polyfurans’,[34] or ‘pseudolignin’.[35,36] Interestingly, pseudolignin was not formed at L/S=8 even at the very high severity.

The L/S reduction from 8 to 4 decreases the amount of SL by 50% to a rather low SL yield (about 7%). The yield of AEL goes through a maximum at the reaction temperature of 195˚C, achieving about 90% of the original biomass lignin (**Figure 3b**). Accordingly, the amount of RL was minimal at T=195˚C. However, due to high formation of pseudolignin under these conditions, also the amounts of RL were also significant.

The reaction temperature of 195˚C resulted in maximum yields of AEL (L/S=4) and it was selected to elucidate the effect of process severity (P-factors ranging from 500 to 2500) under these conditions.

Effect of P-factor. Regarding the extracted solids composition at 195˚C and L/S=4 (**Figure 4a**), the content of glucan was in the range of 60%, with highest value of 71% at P-factor=2000. Xylan contents (4-1.6%) were lower than in the first set of experiments (L/S=8). In contrast, the lignin content was higher (26-37%) than that at L/S=8.

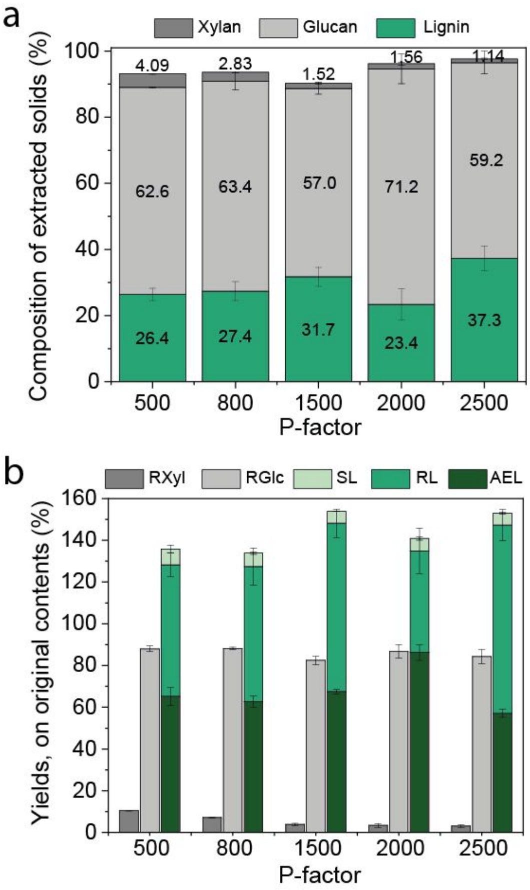

Figure 4. Effect of P-factor at L/S=4 and 195˚C on the (a) composition of extracted solids (b) yields measured in the extracted-solids for RGlc, RXyl and RL. The yields of AEL and SL (in hydrolysate) are also included. All the values were calculated based on the respective content in the original wood feedstock.

The yields of RXyl expectedly decreased with increasing P-factor, from 10% at P=500 to 3% at P=2500. The amount of RGlc was in the range of 82-88% (**Figure 4b**).

Similarly to results discussed earlier (**Fig. 3b),** the total amount of lignin (together with pseudolignin) was surprisingly very high even at a rather low P-factor of 500 and did not increase significantly as the reaction continues (**Figure 3,4**). Noteworthy, the amount of AEL obtained after HTT at L/S of 4, 195˚C (**Figure 4b)** was higher as compared to that at L/S of 8 (**Figure 2b)**. The yields of AEL were significant (about 60%) even at low P-factors (**Figure 4b**). Again, the maximal yield of AEL was at P-factor of 2000 with the minimal amount of the RL in the extracted solids. Increased AEL yield is likely associated with lignin depolymerization during HTT and cleavage of lignin-carbohydrate complex (LCC). Further increase in the severity from P-factor of 2000 to 2500 likely results in predominant lignin re-polymerization, the competitive process, and therefore in lower extraction yield due to lower solubility of the re-polymerized lignin.

Low SL amounts (< 7%) were detected in the hydrolysate, regardless the P-factor applied.

In summary, the obtained HTT solids free of hemicellulose but rich in cellulose and contain certain amount of lignin. As has been shown recently,[19,37] biorefinery ligno-cellulose blends can be successfully used for various applications. This approach is rather different from the traditional bioethanol biorefinery approach and collaborates well with the high-purity extracted lignin (AEL) product supplementing it in a potentially integrated biorefinery. A desirable composition and properties of the extracted solids can be obtained by manipulating the process variables.

Characterization of AELs. Considering the high AEL yields in the experimental set at 195˚C and L/S=4, these AELs were subjected to structural analyses.

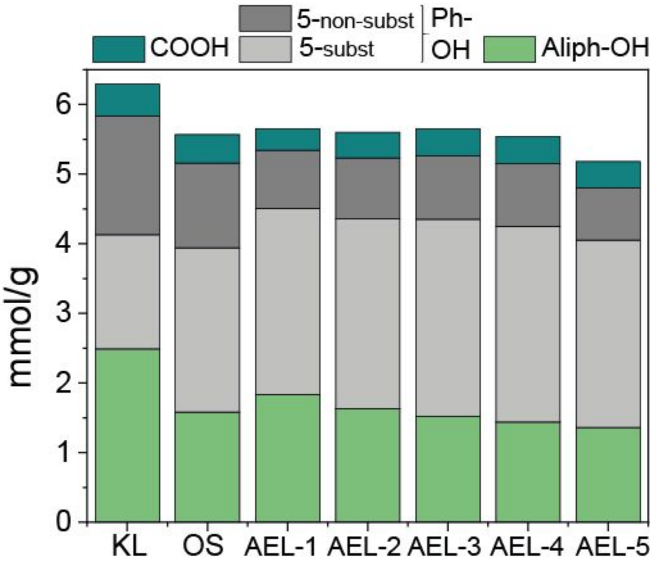

Figure 5. Hydroxyl groups in KL, OS and AEL-(1-5) by ^{31}P NMR.

The analysis of AEL-(1-5) by ^{31}P NMR Spectroscopy (**Figure 5**, **Table S2**) demonstrated approximately similar carboxylic acid (COOH) content, between 0.31-0.38 mmol/g. A gradual and slight increase in phenolic-OH (Ph-OH) content and decrease in aliphatic OH groups (Aliph-OH) were observed when the P-factor was increased to 2000 (AEL-1 to AEL-4), possibly caused by lignin fragmentation. Both types of OH groups were decreased when the P-factor increased to 2500, apparently due to further (secondary) conversion of lignin as well as possible contribution of pseudolignin. However, all differences were rather subtle. Compared to KL, AELs presented lower contents of COOH and Aliph-OH groups and similar content of Ph-OH groups. When compared to a hardwood OS lignin[29] the values were in the same range (**Figure 5**).

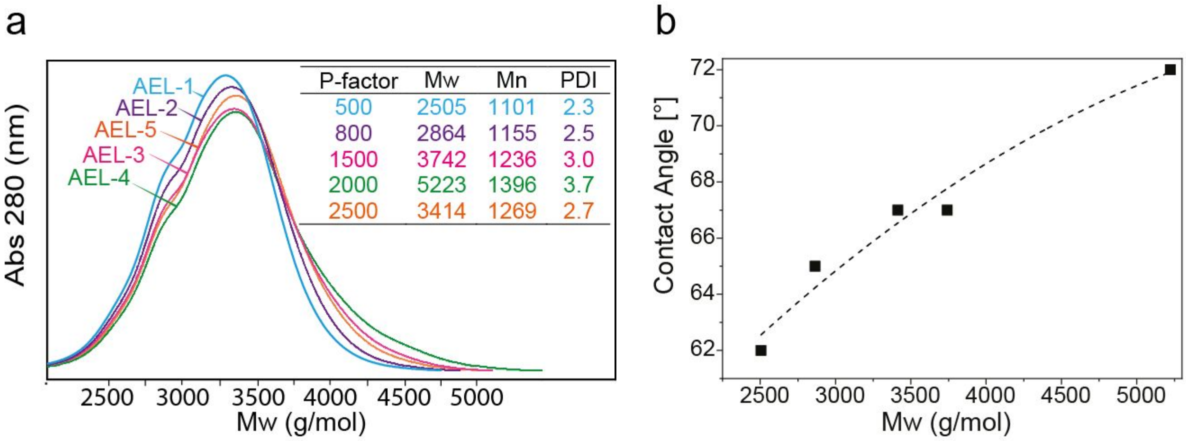

Figure 6. (a) Molecular distributions of AEL and (b) contact angle as a function of average molecular weight (Mw) of AEL.

It should be noted that the calibration using the polystyrene sulphonate do not represent absolute values for lignin molecular weight, but relative ones. However, the method is very common in the area and therefore allows for comparison of our data with others obtained by the similar approach. Moreover, very recently Zinovyev et al.[38] reported a calibration curve allowing converting the relative values from the polystyrene sulphonate calibration to the absolute ones obtained by a cutting-edge method developed by this group.

The molecular weight values (Mw and Mn) and PDI of AEL went through a maximum at P-factor of 2000 **(Figure 6a)**. This indicates higher solubility of lignin fractions in aqueous acetone due to transformation of the original native lignin and possible cleavage of LCC linkages while the P-factor increases up to 2000. Further increase in P-factor to 2500 resulted in a decreased molecular weight, apparently due to decrease in lignin solubility, in which only smaller molecules of the fragmented lignin can be dissolved in the acetone solution. Notably, the MWD correlates with the yield of AEL (**Figure 4b**) indicating that the lignin solubility is the main factor affecting the AEL yield.

The static water contact angles (SCA) from the AELs of different P-factors (**Figure 6b**) did not correlate with the total amount of aliphatic or phenolic hydroxyl groups present in each sample (**Figure 5**). A correlation between SCA and Mw was observed (**Figure 6b**). Therefore, to better understand the relationship between the structural features and the wetting behavior of the AELs, a parallel can be traced with another completely amorphous, water insoluble polymer of comparable wetting behavior, i.e. poly(glycerol adipate) (PGA). The static water contact angles of PGA have been shown to increase from around 58° to 72° at increasing degrees of branching.[39] Branching degree of polymers and water contact angle are two factors that can be correlated due to the reduced accessibility of the hydroxyl functional groups to water molecules. In the case of lignins originated from HTT at increasing degrees of severity, it is known that the cleavage of β-O-4 linkages take place while competitive condensation reactions tend to increase the molecular weight, heterogeneity and, possibly branching/crosslinking.[22,40] Therefore, the molecular weights of the AELs are herein used as a qualitative indicator of such possibly higher degree of branching/crosslinking. Such correlation, however, should be considered with care as, in this specific case, such comparison has only been possible due to the systematic variation of the treatment conditions (and same raw material source), which enabled considerable differences in the degree of condensation and possibly branching without altering considerably the overall amount of hydroxyl groups. Most commonly in previous literature, the static water contact angles of different types of lignins have been compared, yet such association has not been evident given the heterogeneity of the biomass source or processing conditions.

Detailed structural analysis of selected AELs. Based on the obtained results, three samples were chosen for structural analysis by quantitative ^{13}C NMR spectroscopy (**Table 1**, **Figure 7**) and by a semi-quantitative 2D HSQC NMR method (**Figure 8**). Samples AEL 1 and AEL-4 were selected as these materials demonstrated lowest and highest Mw and yield, respectively. In order to investigate the effect of L/S ratio, sample AEL-6 was selected. The results were compared with two technical reference lignins, KL and OS[30] (**Table 1**). The results show that AEL-6 is the less degraded lignin; it has the highest content of native lignin moieties, e.g., oxygenated aliphatic, OMe, β-O-4 structure and the lowest content of degradation products, e.g., CO and COOR moieties, saturated aliphatic carbons, lowest degree of condensation. The higher S/G ratio of AEL-6 than those of AEL-1 and AEL-4 indicates that syringyl (S) units (likely β-O-4 moieties) degrade faster than guaiacyl (G) ones due to their higher reactivity. In contrast to AEL-6, AEL-4 and even AEL-1 are much more degraded, even the latter that was obtained at rather low HTT severity. The difference between AEL-1 and AEL-4 was very subtle (**Table 1**, **Figure 8**).

As the "molecular mass" of an average lignin monomeric unit (M-Ar)[30] was rather close to common values for hardwood lignins (180-230 g/mole), we can hypothesize that the produced pseudolignin did not contribute much into AEL and it was accumulated in the extracted solids (as RL). In addition, ^{13}C and HSQC spectra showed no or small resonances of pseudolignin moieties (compared to those reported earlier, such as carbonyl group of furfural at about 179 ppm and others[38]) in AEL investigated.

Thus, NMR studies suggest that the majority of pseudolignin is accumulated in the extracted solids. Pseudolignin is usually considered as undesirable product of biorefinery.[36] This is apparently true considering the effect of pseudolignin (as well as the true lignin) on enzymatic hydrolysis of pretreated solids. However, in terms of lignin applications, there is no solid evidence of a negative effect of pseudolignin on the application performance. In contrast, organosolv lignins obtained under very severe conditions and containing large amounts of pseudolignins, show better performance than typical organosolv lignins (e.g., Alcell lignin, known as a 'golden lignin standard').[41] Incorporation of furans into the lignin structures may generate additional cross-linking sites (similarly to incorporation of formaldehyde into lignin structure, e.g., in lignin-phenol-formaldehyde formulations) and thus increase lignin reactivity in certain applications, like thermosets. Certainly, this interesting hypothesis needs further experimental confirmation.

Table 1. Quantification of various moieties in AEL and reference technical lignin (KL and OS) by ^{13}C NMR

	KL		OS		AEL-6		AEL-1		AEL-4	
Moieties	per 100Ar	mmol/g	per 100Ar	mmol/g	per 100Ar	mmol/g	per 100Ar	mmol/g	per 100Ar	mmol/g
CO nonconjugated	6	0.35	9	0.48	4	0.21	17	0.83	23	1.24
CO Conjugated	8	0.23	14	0.59	8	0.41	13	0.64	14	0.75
Total CO	15	0.58	29	1.06	12	0.62	30	1.47	37	1.99
COOR nonconjugated	15	0.92	17	0.48	10	0.51	15	0.74	16	0.86
COOR conjugated	2	0.06	4	0.11	2	0.10	2	0.10	3	0.16
Total COOR	17	0.98	21	0.59	12	0.62	17	0.83	19	1.02
OMe	81	4.73	103	6.23	136	7.00	108	5.29	97	5.22
S/G ratio	na	na	1.18		2.31		1.55		1.36	
ArH	234	12.75	202	9.80	201	10.34	187	9.17	183	9.84
DC, %	66		44		17		37		43	
Oxygen. Aliphatic	93	4.61	82	5.96	160	8.23	104	5.10	79	4.25
Saturated Aliphatic	109	6.40	149	4.74	83	4.27	150	7.35	122	6.56
Side Chain Length	233	12.57	281	12.35	267	13.73	301	14.75	257	13.82
β-O-4 (total)	7	0.29	7	0.37	28	1.44	9	0.44	4	0.22
Carbohydrates	~1	0.17	<1		~1		<1		<1	
M-Ar, g/mole	173		178		194		204		186	

na: not applicable; DC: degree of condensation; M-Ar: "molecular mass" values of an averaged lignin monomeric unit

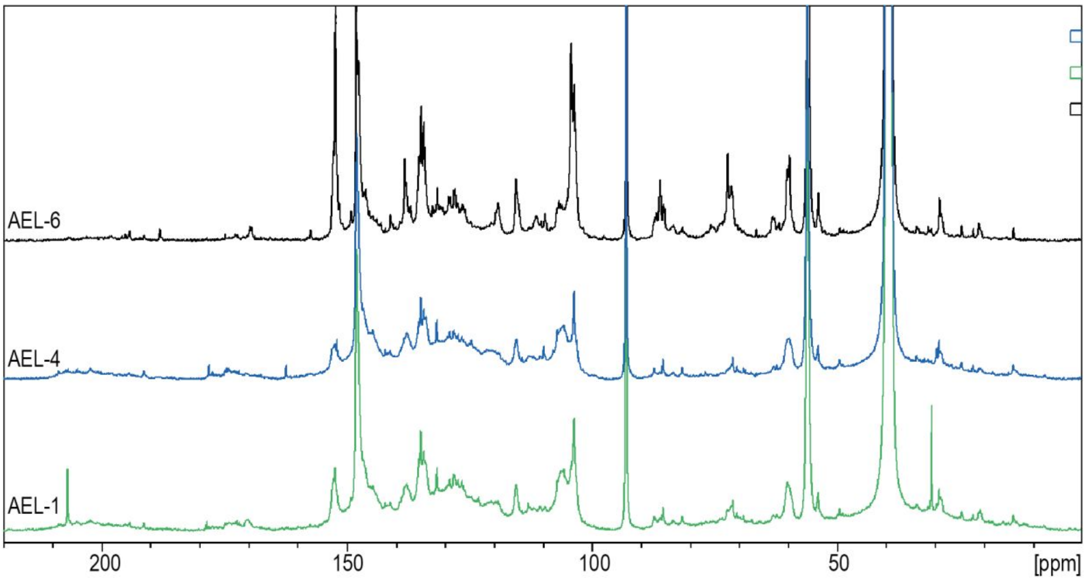

Figure 7. ^{13}C NMR spectra of AEL-1 and AEL-4 (from L/S= 4) and AEL-6 (from L/S=8).

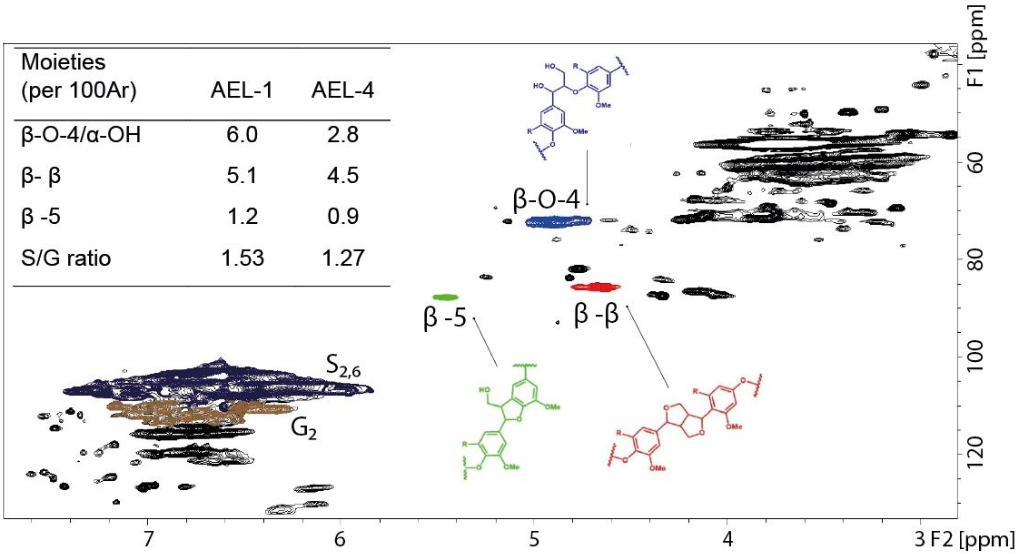

Moieties (per 100Ar)	AEL-1	AEL-4
β-O-4/α-OH	6.0	2.8
β- β	5.1	4.5
β -5	1.2	0.9
S/G ratio	1.53	1.27

Figure 8. HSQC spectrum of AEL-1 and the quantification of AEL-1 and AEL-4 of various moieties by a combination of ^{13}C and HSQC NMR methods.

Controlled drying of AEL into lignin micro and nanoparticles (LMNP). Efforts related to the industrial production of lignin conventionally involve a final drying step via spray drying of the extracted lignin suspension. Morphological and dimensional control, however, are not usually taken into consideration, whereas the powder has a wide size distribution in the micrometer range and poorly defined shape characteristics. Most often, these factors limit the direct utilization of such dry lignin for any commercial application. In fact, further processing involving dissolution of the lignin is most often required. In contrast, nano- and micro-particles in the colloidal size range and having controllable morphologies are highly sought after especially because of the emerging properties arising at such length-scale. The behavior of colloids in suspension, for instance, is much less affected by gravitational forces than particles of several microns, especially in the case of low-density materials.[42] For this reason, suspensions of colloidal lignin having intermediate wetting properties can be used to create stable Pickering emulsions[32] that may not be achieved using particles of several microns. Furthermore, by decreasing the particle size and consequently increasing the surface area to volume ratio, surface and near surface properties become increasingly relevant. Various applications can thus benefit from colloidal particles, such as in paintings and coatings, adhesives, emulsions, rheology modifiers, antimicrobial agents and many others.[43] Therefore, in this work, AEL was used to exemplify the convenience of incorporating an aerosol-flow reactor in the final recovery / evaporation step for the direct production of spherical, dry LMNP. Diverse applications of such particles have been identified in recent years,[44–47] indicating the advantage of having a controllable process integrated to the production of lignin in biorefineries or pulp mills.

For the preparation and characterization of LMNP, the AEL of higher yield (P-factor 2000, 195˚C and L/S = 4) was selected and compared to kraft lignin, which has been previously used for particle fabrication through aerosol-flow. Acetone-water solvents, however, is used for the first time in such aerosol-flow method, offering a promising alternative to associated techno-economical considerations. In short, the aerosol-flow reactor produces LMNP by a controlled drying process which can be divided in different stages (**Figure 9a**). First, the lignin suspension is atomized and carried upwards under a laminar flow at a controlled temperature. In this stage, the solid spherical particles are formed. Then, a turbulent flow is introduced in the system for further removal of the residual solvent. At the end of the process, the particles are size-screened and recovered in collectors. Here, two fractions were used, with size distributions shown in **Figure 9d,e**. The size histograms were fit to a log-normal function, reporting mean sizes of ca. 489 and 606 nm for the small and large fractions, respectively. Despite of the similar mean particle size, the small fraction presented only ca. 6 % of the particles larger than 1 μm (upper limit of the colloidal range), while the large fraction had ca. 15 %. The largest particle size for each fraction was the most striking difference between the two populations: the upper limit for the small and the large fraction was ca. 2 μm and 15 μm, respectively.

The surface morphology (**Figure 9b,c**) tended to change for larger particles as crumpling effects were more predominant. Wrinkled and crumpled kraft lignin particles have been previously produced by using a blowing agent,[48] whereas in the present case no additives were needed. The zeta potential of the acetone extracted LMNP was -35 mV (small size fraction), lower than that measured for kraft LMNP of equivalent size, -50 mV (**Figure 9f**). This result points to a higher colloidal stability in aqueous media for the kraft lignin particles and also correlate with the contact angle values previously discussed, pointing to the lower hydrophilicity of AEL particles.

LMNP have extensive potential applications that can benefit from our process.[49] For instance, the more hydrophilic fractions can find use in applications where colloidal stability in water is important, while the less hydrophilic particles are suitable for better compatibility with hydrophobic components.

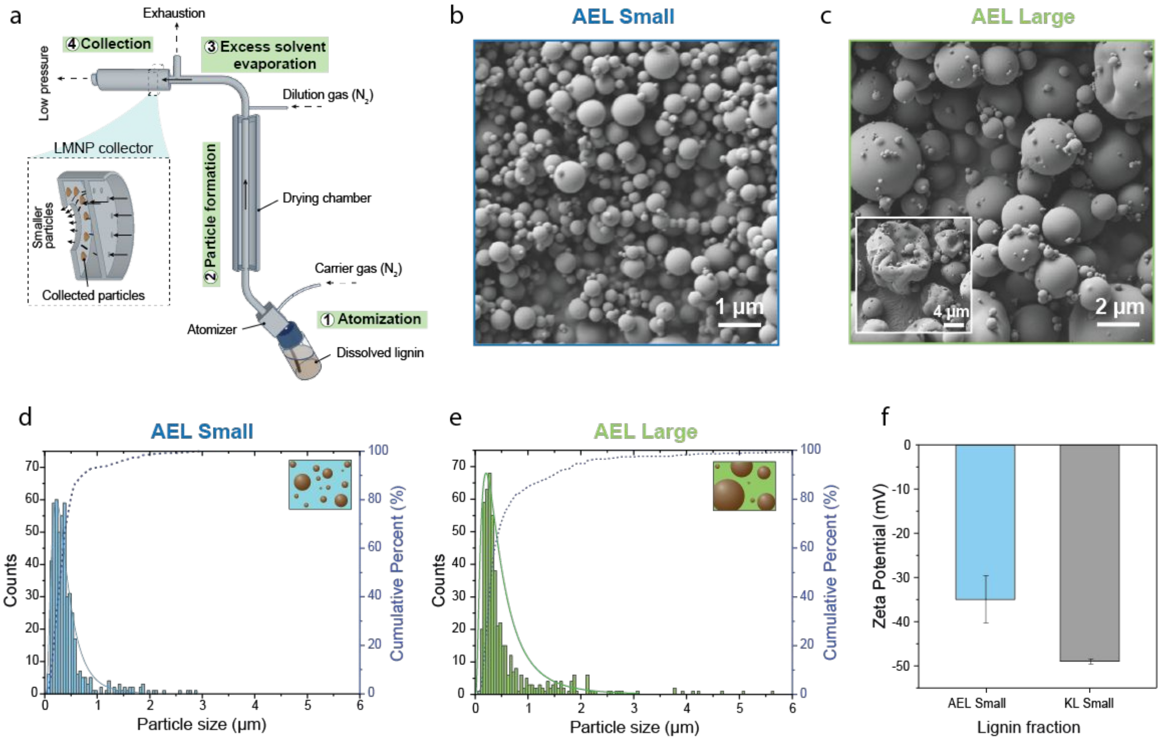

Figure 9. (a) Aerosol-flow reactor set up for the synthesis of LMNP. SEM of LMNP at (b) small and (c) large fractions. Particle size distribution of LMNP at (d) small and (e) large fractions. (f) Zeta potential of LMNP and a comparative common kraft lignin (KL) at fraction small.

In a previous estimation of the theoretical manufacturing costs for LMNP by aerosol-flow reactor, the use of a biorefinery lignin and acetone as solvent were raised as potential precursors.[49] In that work, the estimated manufacturing cost of lignin particles produced from a kraft lignin at 2% concentration, as previously reported,[32,49] was 1750 US\$ t^{-1}. While, the manufacturing cost of a biorefinery lignin in acetone at 5% concentration would cost 58% less (747 US\$ t^{-1}).[49] Importantly, we observed in practice that no heating of the reactor was required for the drying of the particles when using acetone as the solvent. In fact, the particles were produced at room temperature (ca. 25 ˚C). We demonstrated herein that the production of LMNP from a biorefinery lignin in acetone is suitable and allows a higher concentration of 5% in the precursor solution. In addition, the LMNP presented unique properties while a dramatic reduction of manufacturing costs can be achieved.

Overall, we believe that our new biorefinery approach suggests application of all process streams for high-value products in contrast to the traditional current biorefinery focused on the bioethanol or monomeric sugars only. The focus of the current research was in elucidation of the effect of the HTT conditions on the yield and the structure of the extracted lignins as the first step of the alternative biorefinery. We found the maximal AEL yield at rather severe conditions, but it is not necessarily the optimal condition for lignin valorization; this would be also dependent on the required lignin characteristics (e.g., less degraded lignin may be desirable even at a lower yield).

We believe that the new approach may be easily incorporated into the traditional bioethanol biorefinery. Although the operation conditions were more severe than traditionally used in the sugar-based biorefinery, the extracted solids still can be used for monomeric sugar (specifically glucose) production by enzymatic hydrolysis. We have not investigated their reactivity comprehensively yet, but our preliminary results indicate (paper in preparation) that the glucose yield was rather similar or even higher than that from the solids produced under traditional HTT conditions (at P-factor of about 800).[33,50,51]

Alternatively (and ideally) extracted lignocellulosic solids can be used for other high-value applications suggested very recently[19] in particular when a synergism between lignin and cellulose is expected. Furthermore, the extracted HTT solids may be utilized for consequent hydrotermolysis[52] where the presence of pseudolignin in the solids, discussed earlier, may be beneficial for a higher yield of the biochar produced.

The decision on the best integrated biorefinery approach will be made after understanding the process-structure-properties correlations for all biorefinery streams and also considering economic aspects (e.g., the production costs, yields and potential values of the products).

CONCLUSIONS

A simple, green and affordable process for biomass conversion was presented in this work as a new biorefinery approach for HTT. Overall, it suggests application of all process streams for high-value products in contrast to the traditional current biorefinery, focused on the bioethanol or monomeric sugars only, by operating in a new range of HTT conditions. In the current research, we studied the effect of HTT conditions on the yields and characteristics of extracted lignins. High purity lignins of high yields (up to ca 90% per original biomass lignin) were successfully extracted from hydrothermal treated solids under ambient conditions. By varying HTT conditions, we were able to control lignin yields and properties. More specifically, the chemical structure and molecular mass of the lignin could be tailored by the selection of the process variables. For example, the average molecular mass (Mw) of the isolated lignins was in the range of 2.5 - 5 kDa while the amount of β-O-4 linkages was 4-28 per 100 Ar. Significant reduction in manufacturing costs (by 58 %) of lignin particles by aerosol-flow method were achieved when the biorefinery lignin was used in a LMNP integrated production process. Our biorefinery approach brings an alternative to lignin valorization while the extracted-solids (cellulose-rich fraction) can be considered for integration in potential materials for emerging applications or/and as a feedstock for traditional bioethanol production.

ASSOCIATED CONTENT

Supporting Information. The following files are available free of charge.
Chemical composition of feedstock and generated products; ^{31}P NMR of acetone-extracted lignin, severity factor and profile of hydrothermal treatments (PDF).

AUTHOR INFORMATION

Corresponding Author

*E-mail: mikhail.balakshin@aalto.fi

Notes

The authors declare no competing financial interest.

ACKNOWLEDGMENT

The work was a part of the Academy of Finland Flagship's programme (Competence Center for Materials Bioeconomy, FinnCERES). The authors acknowledge Atte Mikkelson for the composition analytics and SEC measurements. L. Greca acknowledges NordForsk project (LIFT) and funding by School of Chemical Engineering for scholarship.

REFERENCES

(1) Maity, S. K. Opportunities, Recent Trends and Challenges of Integrated Biorefinery: Part I. *Renew. Sustain. Energy Rev.* **2015**, *43*, 1427–1445. https://doi.org/10.1016/J.RSER.2014.11.092

(2) Chatterjee, S.; Saito, T. Lignin-Derived Advanced Carbon Materials. *ChemSusChem* **2015**, *8* (23), 3941–3958. https://doi.org/10.1002/cssc.201500692

(3) Jørgensen, H.; Kristensen, J. B.; Felby, C. Enzymatic Conversion of Lignocellulose into Fermentable Sugars: Challenges and Opportunities. *Biofuels, Bioprod. Biorefining* **2007**, *1*, 119–134. https://doi.org/10.1002/BBB

(4) Aslanzadeh, S.; Ishola, M. M.; Richards, T.; Taherzadeh, M. J. An Overview of Existing Individual Unit Operations. *Biorefineries* **2014**, 3–36. https://doi.org/10.1016/B978-0-444-59498-3.00001-4

(5) Carvalheiro, F.; Duarte, L. C.; Gírio, F. M. Hemicelluloses Biorefinery: A Review on Biomass Pretreatments. *J. Sci. Ind. Res. (India).* **2008**, *67* (November), 849–864.

https://doi.org/10.1016/j.talanta.2015.06.045

(6) Jeong, S.-Y.; Lee, J.-W. Hydrothermal Treatment. In *Pretreatment of biomass: processes and technologies*; Pandey, A., Negi, S., Binod, P., Larroche, C., Eds.; 2015; pp 61–74.

(7) Hao, N.; Lu, K.; Ben, H.; Adhikari, S.; Lacerda, T. B.; Ragauskas, A. J. Effect of Autohydrolysis Pretreatment Conditions on Sugarcane Bagasse Structures and Product Distribution Resulting from Pyrolysis. *Energy Technol.* **2018**, *6* (4), 640–648. https://doi.org/10.1002/ente.201700490

(8) Fatehi, P.; Ni, Y. Integrated Forest Biorefinery – Prehydrolysis/Dissolving Pulping Process. In *Sustainable Production of Fuels, Chemicals, and Fibers from Forest Biomass*; ACS Symposium Series; American Chemical Society, 2011; Vol. 1067, pp 18–475. https://doi.org/doi:10.1021/bk-2011-1067.ch018

(9) Borrega, M.; Larsson, P. T.; Ahvenainen, P.; Ceccherini, S.; Maloney, T.; Rautkari, L.; Sixta, H. Birch Wood Pre-Hydrolysis vs Pulp Post-Hydrolysis for the Production of Xylan-Based Compounds and Cellulose for Viscose Application. *Carbohydr. Polym.* **2018**, *190* (October 2017), 212–221. https://doi.org/10.1016/j.carbpol.2018.02.064

(10) Venkateswar Rao, L.; Goli, J. K.; Gentela, J.; Koti, S. Bioconversion of Lignocellulosic Biomass to Xylitol: An Overview. *Bioresour. Technol.* **2015**, *213*, 299–310. https://doi.org/10.1016/j.biortech.2016.04.092

(11) Fujimoto, S.; Inoue, S.; Yoshida, M. High Solid Concentrations during the Hydrothermal Pretreatment of Eucalyptus Accelerate Hemicellulose Decomposition and Subsequent Enzymatic Glucose Production. *Bioresour. Technol. Reports* **2018**, *4* (July), 16–20. https://doi.org/10.1016/j.biteb.2018.09.006

(12) Pontes, R.; Romaní, A.; Michelin, M.; Domingues, L.; Teixeira, J.; Nunes, J. Comparative Autohydrolysis Study of Two Mixtures of Forest and Marginal Land Resources for Co-Production of Biofuels and Value-Added Compounds. *Renew. Energy* **2018**, *128*, 20–29. https://doi.org/10.1016/j.renene.2018.05.055

(13) Gallina, G.; Cabeza, Á.; Biasi, P.; García-Serna, J. Optimal Conditions for Hemicelluloses Extraction from Eucalyptus Globulus Wood: Hydrothermal Treatment in a Semi-Continuous Reactor. *Fuel Process. Technol.* **2016**, *148*, 350–360. https://doi.org/10.1016/J.FUPROC.2016.03.018

(14) Pronyk, C.; Mazza, G.; Tamaki, Y. Production of Carbohydrates, Lignins, and Minor Components from Triticale Straw by Hydrothermal Treatment. *J. Agric. Food Chem.* **2011**, *59* (8), 3788–3796. https://doi.org/10.1021/jf104543a

(15) Leppänen, K.; Spetz, P.; Pranovich, A.; Hartonen, K.; Kitunen, V.; Ilvesniemi, H. Pressurized Hot Water Extraction of Norway Spruce Hemicelluloses Using a Flow-through System. *Wood Sci. Technol.* **2011**, *45* (2), 223–236. https://doi.org/10.1007/s00226-010-0320-z

(16) Berlin, A.; Balakshin, M. Y. Industrial Lignins: Analysis, Properties, and Applications. In *Bioenergy Research: Advances and Applications*; Gupta, V. K., Kubicek, C. P., Saddler, J., Xu, F., Tuohy, M., Eds.; Elsevier: Amsterdam, Nederlands, 2014; pp 315–336.

(17) Holladay, J. E.; White, J. F.; Bozell, J. J.; Johnson, D. Top Value-Added Chemicals from Biomass - Volume II - Results of Screening for Potential Candidates from Biorefinery Lignin. *Department of Energy*. US 2007.

(18) Ragauskas, A. J.; Beckham, G. T.; Biddy, M. J.; Chandra, R.; Chen, F.; Davis, M. F.; Davison, B. H.; Dixon, R. a; Gilna, P.; Keller, M.; et al. Lignin Valorization: Improving Lignin Processing in the Biorefinery. *Science* **2014**, *344* (6185), 1246843. https://doi.org/10.1126/science.1246843

(19) Balakshin, M.; Capanema, E. A.; Huang, Z.; Sulaeva, I.; Rojas, O.; Feng, M.; Rosenau, T.; Potthast, A. Recent Achievement in the Valorization of Technical Lignins. In *The 8th Nordic Wood Biorefinery Conference: NWBC 2018*; Hytönen Eemeli, V. J., Ed.; Helsinki, Finland, 2018; pp 151–156.

(20) Strassberger, Z.; Tanase, S.; Rothenberg, G. The Pros and Cons of Lignin Valorisation in an Integrated Biorefinery. *RSC Adv.* **2014**, *4* (48), 25310–25318. https://doi.org/10.1039/c4ra04747h

(21) Sun, S.; Cao, X.; Sun, S.; Xu, F.; Song, X.; Sun, R. C.; Jones, G. L. Improving the Enzymatic Hydrolysis of Thermo-Mechanical Fiber from Eucalyptus Urophylla by a Combination of Hydrothermal Pretreatment and Alkali Fractionation. *Biotechnol. Biofuels* **2014**, *7* (1), 1–12. https://doi.org/10.1186/s13068-014-0116-8

(22) Li, J.; Henriksson, G.; Gellerstedt, G. Lignin Depolymerization/Repolymerization and Its Critical Role for Delignification of Aspen Wood by Steam Explosion. *Bioresour. Technol.* **2007**, *98* (16), 3061–3068. https://doi.org/10.1016/J.BIORTECH.2006.10.018

(23) Lora, J. H.; Wayman, M. Delignification of Hardwoods by Atohydrolysis and Extraction. *Tappi* **1978**, *61* (6), 47–50.

(24) Tian, D.; Hu, J.; Bao, J.; Chandra, R. P.; Saddler, J. N.; Lu, C. Lignin Valorization: Lignin Nanoparticles as High-Value Bio-Additive for Multifunctional

Nanocomposites. *Biotechnol. Biofuels* **2017**, *10* (1), 1–11. https://doi.org/10.1186/s13068-017-0876-z

(25) Lievonen, M.; Valle-Delgado, J. J.; Mattinen, M. L.; Hult, E. L.; Lintinen, K.; Kostiainen, M. A.; Paananen, A.; Szilvay, G. R.; Setälä, H.; Österberg, M. A Simple Process for Lignin Nanoparticle Preparation. *Green Chem.* **2016**, *18* (5), 1416–1422. https://doi.org/10.1039/c5gc01436k

(26) Sixta, H. Kraft Pulping Kinetics. In *Handbook of Pulp*; Wiley-VCH: Weinheim, Germany, 2006; pp 185–365.

(27) Goldschmid, O. Ultraviolet Spectra. In *Lignins: Occurrence, Formation, Structure and Reactions.*; Sarkanen, K.V., Ludwig, C. H., Ed.; New York, 1971; pp 241–298.

(28) Granata, A.; Argyropoulos, D. . 2-Chloro-4,4,5,5-Tetramethyl-1,3,2-Dioxaphospholane, a Reagent for Theaccurate Determination of the Uncondensed and Condensed Phenolic Moietiesin Lignins. *J. Agric. Food Chem.* **1995**, *43*, 1538–1544. https://doi.org/10.1021/jf00054a023

(29) Balakshin, M.; Capanema, E. On the Quantification of Lignin Hydroxyl Groups with ^{31}P and ^{13}C NMR Spectroscopy. *J. Wood Chem. Technol.* **2015**, *35* (3), 220–237. https://doi.org/10.1080/02773813.2014.928328

(30) Balakshin, M. Y.; Capanema, E. A. Comprehensive Structural Analysis of Biorefinery Lignins with a Quantitative 13C NMR Approach. *RSC Adv.* **2015**, *5* (106), 87187–87199. https://doi.org/10.1039/c5ra16649g

(31) Zhang, L.; Gellerstedt, G. Quantitative 2D HSQC NMR Determination of Polymer Structures by Selecting Suitable Internal Standard References. *Magn. Reson. Chem.* **2007**, *45* (2007), 37–45. https://doi.org/10.1002/mrc

(32) Ago, M.; Huan, S.; Borghei, M.; Raula, J.; Kauppinen, E. I.; Rojas, O. J. High-Throughput Synthesis of Lignin Particles (~30 Nm to ~2 Mm) via Aerosol Flow Reactor: Size Fractionation and Utilization in Pickering Emulsions. *ACS Appl. Mater. Interfaces* **2016**, *8* (35), 23302–23310. https://doi.org/10.1021/acsami.6b07900

(33) Borrega, M.; Tolonen, L. K.; Bardot, F.; Testova, L.; Sixta, H. Potential of Hot Water Extraction of Birch Wood to Produce High-Purity Dissolving Pulp after Alkaline Pulping. *Bioresour. Technol.* **2013**, *135*, 665–671. https://doi.org/10.1016/j.biortech.2012.11.107

(34) Khol'kin, T. *The Technology of the Wood' Hydrolysis Industries*; Lesnaya promyshlennost (in Russian): Moscow, 1989.

(35) Li, J.; Henriksson, G.; Gellerstedt, G. Carbohydrate Reactions during High-

Temperature Steam Treatment of Aspen Wood. *Appl. Biochem. Biotechnol. - Part A Enzym. Eng. Biotechnol.* **2005**, *125* (3), 175–188. https://doi.org/10.1385/ABAB:125:3:175

(36) Hu, F.; Jung, S.; Ragauskas, A. Pseudo-Lignin Formation and Its Impact on Enzymatic Hydrolysis. *Bioresour. Technol.* **2012**, *117*, 7–12. https://doi.org/10.1016/j.biortech.2012.04.037

(37) Wang, L.; Ago, M.; Borghei, M.; Ishaq, A.; Papageorgiou, A. C.; Lundahl, M.; Rojas, O. J. Conductive Carbon Microfibers Derived from Wet-Spun Lignin/Nanocellulose Hydrogels. *ACS Sustain. Chem. Eng.* **2019**, *7* (6), 6013–6022. https://doi.org/10.1021/acssuschemeng.8b06081

(38) Zinovyev, G.; Sulaeva, I.; Podzimek, S.; Rössner, D.; Kilpeläinen, I.; Sumerskii, I.; Rosenau, T.; Potthast, A. Getting Closer to Absolute Molar Masses of Technical Lignins. *ChemSusChem* **2018**, *11* (18), 3259–3268. https://doi.org/10.1002/cssc.201801177

(39) Taresco, V.; Creasey, R. G.; Kennon, J.; Mantovani, G.; Alexander, C.; Burley, J. C.; Garnett, M. C. Variation in Structure and Properties of Poly(Glycerol Adipate) via Control of Chain Branching during Enzymatic Synthesis. *Polymer (Guildf).* **2016**, *89*, 41–49. https://doi.org/10.1016/J.POLYMER.2016.02.036

(40) Tolbert, A.; Akinosho, H.; Khunsupat, R.; Naskar, A. K.; Ragauskas, A. J. Characterization and Analysis of the Molecular Weight of Lignin for Biorefining Studies. *Biofuels, Bioprod. Biorefining* **2014**, *8* (6), 836–856. https://doi.org/10.1002/bbb

(41) Berlin, A.; Balakshin, M. Y. Biomass Extraction Process. US2013252292 (A1), 2012.

(42) Dokou, E.; Barteau, M. A.; Wagner, N. J.; Lenhoff, A. M. Effect of Gravity on Colloidal Deposition Studied by Atomic Force Microscopy. *J. Colloid Interface Sci.* **2001**, *240* (1), 9–16. https://doi.org/10.1006/JCIS.2001.7626

(43) Stark, W. J.; Stoessel, P. R.; Wohlleben, W.; Hafner, A. Industrial Applications of Nanoparticles. *Chem. Soc. Rev.* **2015**, *44* (16), 5793–5805. https://doi.org/10.1039/c4cs00362d

(44) Yang, J.; Ching, Y. C.; Chuah, C. H. Applications of Lignocellulosic Fibers and Lignin in Bioplastics: A Review. *Polymers (Basel).* **2019**, *11* (751), 1–26. https://doi.org/10.3390/polym11050751

(45) Beisl, S.; Miltner, A.; Friedl, A. Lignin from Micro- to Nanosize: Production Methods. *Int. J. Mol. Sci.* **2017**, *18* (6), 1244. https://doi.org/10.3390/ijms18061244

(46) Qian, Y.; Deng, Y.; Qiu, X.; Li, H.; Yang, D. Formation of Uniform Colloidal Spheres from Lignin, a Renewable Resource Recovered from Pulping Spent Liquor. *Green Chem.* **2014**, *16*, 2156–2163. https://doi.org/10.1039/c3gc42131g

(47) Yearla, S. R.; Padmasree, K. Preparation and Characterisation of Lignin Nanoparticles: Evaluation of Their Potential as Antioxidants and UV Protectants. *J. Exp. Nanosci.* **2016**, *11* (4), 289–302. https://doi.org/10.1080/17458080.2015.1055842

(48) Kämäräinen, T.; Ago, M.; Seitsonen, J.; Raula, J.; Kauppinen, E. I.; Ruokolainen, J.; Rojas, O. J. Harmonic Analysis of Surface Instability Patterns on Colloidal Particles. *Soft Matter* **2018**, *14* (17), 3387–3396. https://doi.org/10.1039/c8sm00383a

(49) De Assis, C. A.; Greca, L. G.; Ago, M.; Balakshin, M. Y.; Jameel, H.; Gonzalez, R.; Rojas, O. J. Techno-Economic Assessment, Scalability, and Applications of Aerosol Lignin Micro- and Nanoparticles. *ACS Sustain. Chem. Eng.* **2018**, *6* (9), 11853–11868. https://doi.org/10.1021/acssuschemeng.8b02151

(50) Liu, J.; Li, M.; Luo, X.; Chen, L.; Huang, L. Effect of Hot-Water Extraction (HWE) Severity on Bleached Pulp Based Biorefinery Performance of Eucalyptus during the HWE-Kraft-ECF Bleaching Process. *Bioresour. Technol.* **2015**, *181*, 183–190. https://doi.org/10.1016/j.biortech.2015.01.055

(51) Borrega, M.; Niemela, K.; Sixta, H. Effect of Hydrothermal Treatment Intensity on the Formation of Degradation Products from Birchwood. *Holzforschung* **2013**, *67* (8), 871–879. https://doi.org/10.1515/hf-2013-0019

(52) Siipola, V.; Tamminen, T.; Källi, A.; Lahti, R.; Romar, H.; Rasa, K.; Keskinen, R.; Hyväluoma, J.; Hannula, M.; Wikberg, H. Effects of Biomass Type, Carbonization Process, and Activation Method on the Properties of Bio-Based Activated Carbons. *BioResources* **2019**, *13* (3), 5976–6002. https://doi.org/10.15376/biores.13.3.5976-6002

BRIEFS

Green and simple lignin-centered biorefinery process based on hydrothermal treatment integrated with low-cost synthesis of lignin micro/nanoparticles.

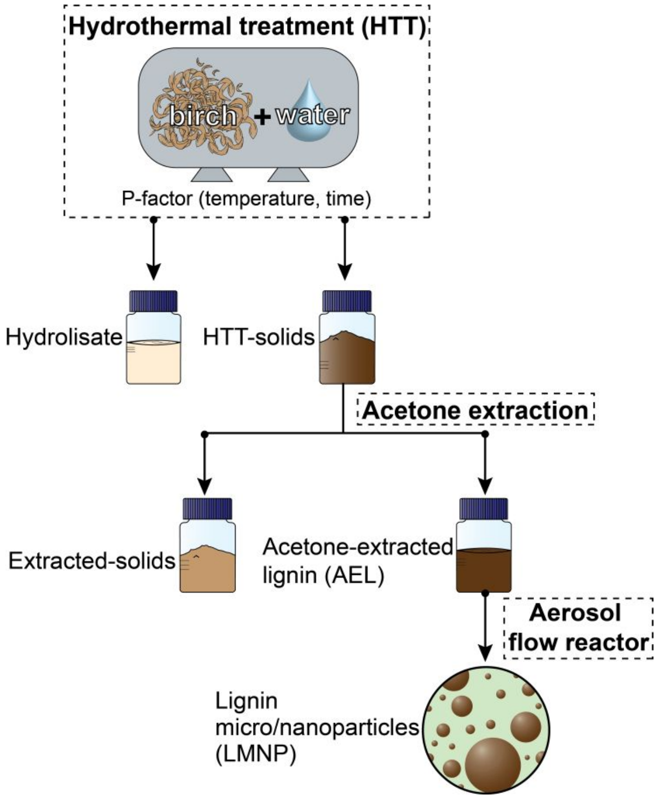

For Table of Contents Use Only